

Supplementary Information

Insight into the origin of carbon corrosion in positive electrodes of supercapacitors

Rui Tang, Kaishi Taguchi, Hiroto Nishihara*, Takafumi Ishii, Emilia Morallón, Diego Cazorla-Amorós, Toshihiro Asada, Naoya Kobayashi, Yasuji Muramatsu and Takashi Kyotani

1. Fabrication of anthracite-derived activated carbon (AAC)

Spanish anthracite was ground and sieved to a particle size of 600 to 1000 μm . The resulting powder (2 g) was mixed with 10 ml of KOH aqueous solution (the ratio is KOH:anthracite = 4:1) and the mixture was stirred at 60 $^{\circ}\text{C}$ for 2 h. The slurry thus obtained was dried in an oven at 110 $^{\circ}\text{C}$ overnight. Then, the sample was heat treated in a horizontal furnace at 700 $^{\circ}\text{C}$ for 1 h (heating rate is 5 $^{\circ}\text{C min}^{-1}$).

2. Nanoporosity

Table S1. Textural properties of carbon samples.

Sample	S_{BET} ($\text{m}^2 \text{ g}^{-1}$)	$V_{50\text{nm}}^a$ ($\text{cm}^3 \text{ g}^{-1}$)	V_{t}^b ($\text{cm}^3 \text{ g}^{-1}$)	V_{micro}^c ($\text{cm}^3 \text{ g}^{-1}$)	V_{meso}^d ($\text{cm}^3 \text{ g}^{-1}$)	V_{macro}^e ($\text{cm}^3 \text{ g}^{-1}$)
rGO	369	0.47	0.48	0.13	0.34	0.01
XC72	220	0.35	1.35	0.09	0.26	1.00
DB	732	0.90	1.76	0.29	0.61	0.86
KB	767	0.80	1.62	0.27	0.53	0.82
BP	1341	1.44	3.10	0.54	0.90	1.66
YP50F	1708	0.79	0.82	0.73	0.06	0.03
AAC	3650	2.15	2.18	1.34	0.81	0.03
AACH2	3318	2.01	2.04	1.24	0.77	0.03
ZTC	3598	1.67	1.91	1.52	0.15	0.24

^a Pore volume for pores less than 50 nm, which is calculated from the N₂ adsorption amount at $P/P_0 = 0.96$.

^b Total pore volume calculated from the N₂ adsorption amount at $P/P_0 = 0.99$.

^c Micropore volume calculated by the Dubinin-Radushkevitch method.

^d Mesopore volume calculated by $V_{\text{meso}} = V_{50\text{nm}} - V_{\text{micro}}$.

^e Macropore volume calculated by $V_{\text{macro}} = V_{\text{t}} - V_{50\text{nm}}$. Note that V_{macro} covers only a part of macropore volume which can be detected by N₂ adsorption at -196°C .

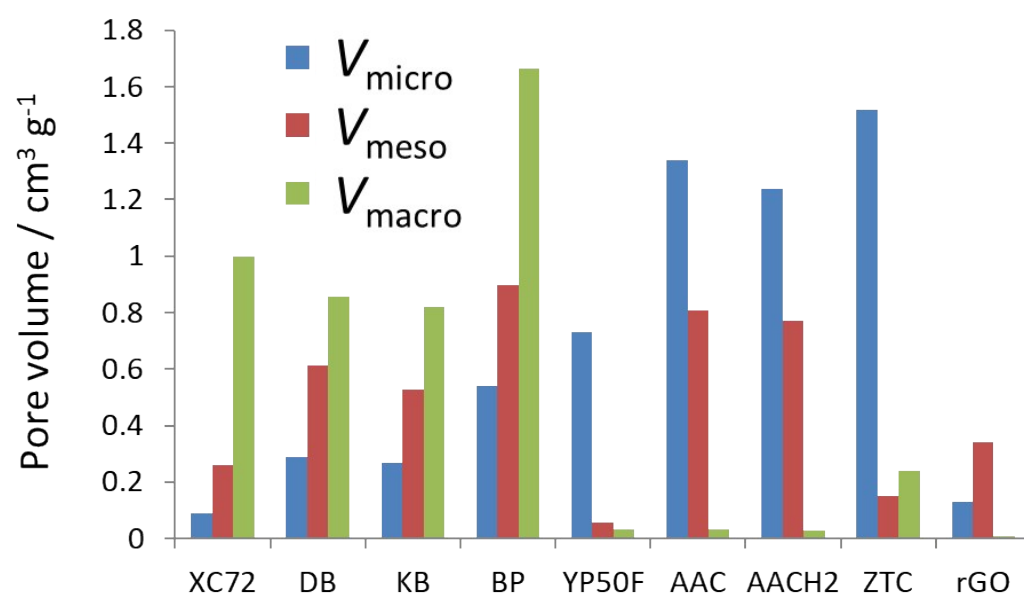


Fig. S1 Compositions of micro/meso/macropore volumes of carbon samples.

3. Crystallinity

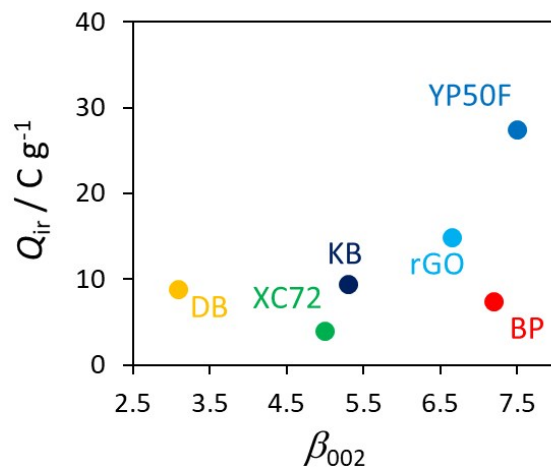


Fig. S2 The plot of Q_{ir} against the FWHM of the carbon 002 peak. AAC, AACH2, and ZTC are not plotted because they show no 002 peak.

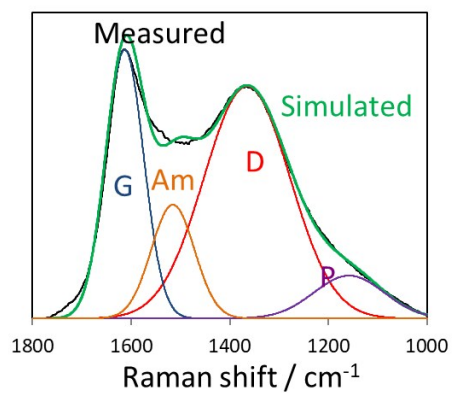


Fig. S3 Curve-fitting result of AAC Raman spectra.

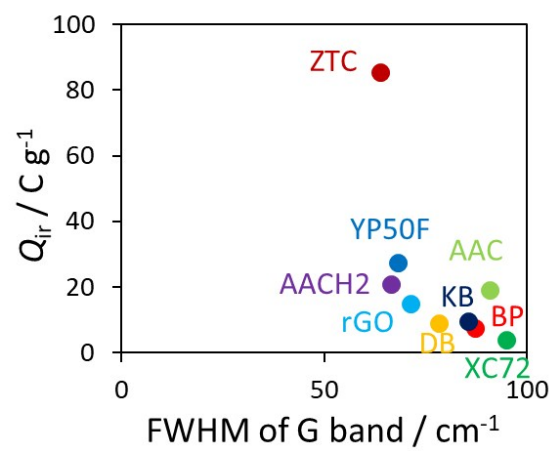


Fig. S4 The plot of Q_{ir} against the FWHM of the carbon G-band.

4. Spin/H-terminated edge sites ratio

Table S2 shows the ratios of spin density to the number of H-terminated edge sites for all samples. The spin density is measured by magnetic susceptibility measurement with the assumption that $S = 1/2$. The amount of H-terminated edge sites were calculated by using the data of desorbed H_2 during TPD measurements. Here we assume that 1 mole of desorbed H_2 originates from 2 moles of H-terminated edge sites.

Table S2. The ratios of spin to H-terminated edge sites (calculated by using the amount of desorbed H_2 gas during TPD measurement).

Sample	Spin density ($\times 10^{20}$ spin g^{-1})	Number of H-terminated edge sites ($\times 10^{20}$ g^{-1})	Ratio of spin to H-terminated edge sites
YP50F	0.71	25.5	2.8%
ZTC	0.98	73.3	1.3%
AAC	1.5	8.62	17.4%
AACH2	1.2	17.9	6.7%
DB	0.15	5.37	2.8%
KB	0.15	11.8	1.3%
XC72	0.091	4.92	1.8%
BP	0.15	7.71	2.1%

5. Coefficient of determination (R^2).

In Fig. 7, a coefficient of determination (R^2) is calculated by the following equation:

$$R^2 = 1 - \frac{\sum_i (y_i - f_i)^2}{\sum_i (y_i - \bar{y})^2} \quad (1)$$

where y_i is the data set, \bar{y} is the mean of the observed data, f_i is a predicted value associated with each y_i . For an ideal linear correlation, the value of R^2 becomes 1.